Multi-fluid model applied to calculate backmixing and mass transfer in bubble columns

D. Wiemann, D. Mewes,
Institute of Process Engineering, University of Hannover,
Callinstr. 36, 30167 Hannover, Germany,
e-mail: dms@ifv.uni-hannover.de

Abstract

For the calculation of reactive flows in bubble columns the local interfacial area is one of the key parameters. In addition backmixing causes a residence time distribution in the gas and liquid phase, thus mixing phenomena have to be considered as well. The three-dimensional, instationary flow fields in bubble columns are numerically calculated using an Euler multi-fluid model. The resulting set of equations enables the simultaneous calculation of mass transfer and backmixing in the gas and liquid phase. Therefore the local bubble size is calculated in dependence of the flow field using a transport equation for the mean bubble volume. A perfect tracer is added into both the gaseous and the liquid phase. From the calculations the time-dependent concentration fields are obtained. Assuming the one-dimensional dispersion model the axial dispersion coefficients are calculated. The dispersion coefficients for the gas and liquid phase are in good agreement with experimental investigations of several authors. The multi-fluid model is then extended to consider mass transfer between gas and liquid phases.

Introduction

For the design of bubble column reactors several empirical correlations have been proposed to determine the interfacial area density and backmixing [1], [2]. The conventional design approach is based on these correlations. With increasing computer power computational fluid dynamics is an alternative way to get further insights into the complex two-phase flow. The coupling of population balance equations with computational fluid dynamics enables the calculation of the local interfacial area. In this paper a transport equation for the mean bubble volume originating from a population balance equation approach is coupled with an Euler multi-fluid model. For the calculation of reactive flows not only the interfacial area has to be known but also the mixing properties of the column have to be reasonably predicted. Therefore a perfect tracer is injected into the liquid and the rising bubble swarm to determine backmixing.

Governing equations for bubbly two-phase flow

For the modeling of bubbly flow the Euler-Lagrange and the Euler-Euler approach are common. In addition Direct Numerical Simulations can be applied to calculate the motion of single bubbles and the movement of the gas-liquid interface. For large-scale flows however the Euler-Euler approach is most suitable since it is numerically more efficient than the Euler-Lagrange approach. The Euler approach assumes all phases to be continuously distributed in the computational domain. Therefore also the dispersed gas phase is described by a quasi-continuous fluid. The interphase coupling of the balance equations for mass and momentum is considered by interphase transfer terms. For high superficial gas

velocities the heterogeneous flow regime arises. The enhanced coalescence leads to the formation of a bi-modal bubble size distribution. Therefore the gas phase is described by two interpenetrating phases, which contain the small and the large bubble fraction. Using a multi-fluid approach the governing balance equation for momentum of the i-th phase is

$$\frac{\partial}{\partial t}\left(\alpha_i \rho_i \vec{u}_i\right) + \nabla\left(\alpha_i\left(\rho_i \vec{u}_i \vec{u}_i\right)\right) = -\alpha_i \nabla p_i + \nabla\left(\alpha_i \eta_i \left(\Delta \vec{u}_i + (\Delta \vec{u}_i)^T\right)\right) + \alpha_i \rho_i \vec{g} + \vec{F}_{ij}, \; i=l,1,2; \qquad (1)$$
$$+ S_{break,1-2} + S_{coal,1-2}$$

The index l denotes the liquid phase, 1 and 2 label the small and the large bubble fraction. The terms on the left side of eq. (1) describe the local and convective change of momentum. These terms are balanced by the forces on the right side, namely the forces due to the bulk pressure gradient, viscous shear, gravitational force and the interphase transfer of momentum. The last two terms represent source and sink terms for second order momentum transfer between the small and the large bubble fraction due to bubble coalescence and break-up. Thus these terms only arise in the gas phases. The interphase momentum transfer is mostly influenced by the interphasial drag force. Although additional forces such as lift or added mass forces arise in bubbly flow these forces are neglected here since they play only a minor role following Loth [3] and Joshi [4]. The interphase momentum transfer is calculated to

$$\vec{F}_{il} = C_D \frac{3}{4} \rho_l \frac{\alpha_i}{d_i} \left|\vec{u}_i - \vec{u}_l\right| (\vec{u}_i - \vec{u}_l). \qquad (2)$$

The drag coefficient C_D is calculated following Clift et al. [5] to

$$C_D = \max\left[\frac{24}{Re}(1 + 0.1 Re^{0.75}); \min\left\{\max(0.44, \frac{2}{3} Eo^{1/2}), \frac{8}{3}\right\}\right]. \qquad (3)$$

In eq. (3) the Reynolds- and Eötvös-number are defined as follows:

$$Re_i = \frac{\left|\vec{u}_i - \vec{u}_l\right| d_i}{\nu_l} \qquad (4)$$

$$Eo = \frac{g(\rho_l - \rho_i) d_i^2}{\sigma}. \qquad (5)$$

In eq. (5) the surface tension between the liquid and gas phase is σ. The bubble diameter d_i is calculated from a transport equation for the mean bubble volume. The transport equation for the mean bubble volume of the small and the large bubbles are obtained as given by Lehr et al. [6]. These transport equations are coupled with the balance equations for mass and momentum. The solution of these transport equations also enables the calculation of the Sauter-diameter of the bubble size distribution.

The mass balance equation is written to

$$\frac{\partial(\alpha_i\rho_i)}{\partial t}+\nabla(\alpha_i\rho_i\vec{u}_i)=\dot{M}_{coal,1-2}+\dot{M}_{break,1-2}+\begin{cases}-\dot{M}_{i\to l}, i=1,2\\ +\dot{M}_{j\to l}, i=l;\ j=1,2\end{cases} \tag{6}$$

The first two terms on the right hand side of eq. (6) describe mass transfer between the gas phases due to bubble break-up and coalescence. Therefore they only arise in the gas phases rather than in the liquid phase. The third term considers mass transfer from the gaseous to the liquid phase.
The gas phase consists of two components, which are identical in their properties. In addition to the global mass balance the components mass balances are considered. For the calculation of the mass transfer rate the phase equilibrium at the gas-liquid interface is described following Henry's law. The mass transfer rate is calculated to

$$\dot{m}_{i,l}=\frac{c_l}{c_l-c_{A,l}}\beta_l\left(\rho_{A,pl}-\rho_{A,l}\right) \tag{7}$$

with the bulk molar concentration of the liquid phase c_l and the bulk molar concentration of the transferred component. The mass transfer coefficient is calculated in dependence of a Sherwood-number. For small Reynolds-numbers the bubbles are spherical shaped whereas with increasing Reynolds-number turbulent motions at the surface become more and more important and the bubbles loose their shape. Therefore for small Reynolds-numbers below

$$Re_{crit}=3.73\left(\frac{\rho_l\sigma^3}{g\eta_l^{\,4}}\right)^{0.209}. \tag{8}$$

the Sherwood-number is calculated according to Brauer [7]

$$Sh=Sh_\infty\left[\left(1+0.433\,Re^2\right)^{-1}+0.0000423\right]^{-0.055} \tag{9}$$

with

$$Sh_\infty=2+\frac{0.651(Re\,Sc)^{1.72}}{1+(Re\,Sc)^{1.22}}. \tag{10}$$

For larger Reynolds-numbers the correlation

$$Sh=2+0.015\,Re^{0.89}\,Sc^{0.7} \tag{11}$$

is used instead of eq. (10).

In bubbly two-phase flow the turbulent velocity fluctuations in the liquid phase are caused by the shear induced turbulence as well as due to the presence of bubbles. In this work the influence of the bubbles on the liquid turbulence is described following the proposal of Lopez de Bertodano [8]. The set of equations is solved with the method of finite volumes. Therefore the code CFX-5.7 is used. The computational domain is discretized with a block-

structured grid of hexahedral volumes. The edge length is about 1cm and time-steps of 0.02s are applied. The convective terms are discretized by a second order method.

Dispersion models

Backmixing in the liquid and the gas phase is caused by several mechanisms. The formation of liquid vortices, the occurrence of stagnation zones as well as the turbulent velocity fluctuations cause a residence time distribution in the liquid phase. In addition the coalescence and break-up of bubbles and the non-uniform distribution of the gas phase enhance the formation of a velocity profile in both phases. Coalescence and break-up of bubbles also enhance backmixing in the gaseous phase. For the description of backmixing several models have been developed as summarized by Levenspiel [1]. One of the most popular ones for backmixing in bubble columns is the axial dispersion model, that describes the deviation from ideal plug flow.
The mass flux due to dispersion is described in analogy to molecular transport, although both phenomena differ in their physical nature. In bubbly flow the mass flux due to dispersion is higher than the molecular transport thus the mass balance for a cross sectional element of the bubble column is written to

$$\frac{\partial c}{\partial t} + \frac{j_i}{\alpha_i}\frac{\partial c}{\partial x} = E_{i,ax}\frac{\partial^2 c}{\partial x^2} \quad ,i = g,l \tag{12}$$

neglecting molecular transport and radial dispersion. For a batch operated liquid phase and a pulsewise tracer injection the solution of eq. (12) is approximated by the following summation of infinite terms following Ohki and Inoue [9]

$$\frac{c}{c_\infty} = 1 + 2\sum_{n=1}^{\infty}\left(\cos\left(\frac{n\pi}{H}x\right)\exp\left(-\left(\frac{n\pi}{H}\right)^2 E_{ax,l}t\right)\right). \tag{13}$$

The stationary concentration of the tracer is labeled c_∞, the instantaneous concentration is c. For the practical use of eq. (13) only the first ten terms have to be included. The left side of eq. (13) can be obtained by experiments or as in this work from a numerical calculation of the three-dimensional, instationary flow field. The tracer in the gas phase is injected continuously in the rising bubble swarm. Therefore a sinusoidal tracer inlet concentration is used. The solution of eq. (12) for the case of a sinusoidal input signal leads to the following equation for the axial dispersion coefficient

$$E_{ax,g} = \frac{j_g^3}{\alpha_g^3 \omega^2 H}\ln\left(\frac{c_{in}}{c_{out}}\right). \tag{14}$$

The angular frequency of the sinusoidal input signal is ω, the dispersion height is H, the integral volume fraction of gas is α_g and the superficial gas velocity is j_g. The amplitudes of the tracer concentration are c_{in} at the inlet and c_{out} at the outlet, respectively.

Results

Calculations are performed for three-dimensional, time-dependent flow-fields in cylindrical bubble columns.

In Fig.1 the calculated flow field in a bubble column with 3m height and 40 cm diameter is shown. The liquid streamlines are colored with the specific interfacial area density, the volume fraction of gas and the axial liquid velocity. The superficial gas velocity is 0.1 m/s thus the heterogeneous flow regime is present.

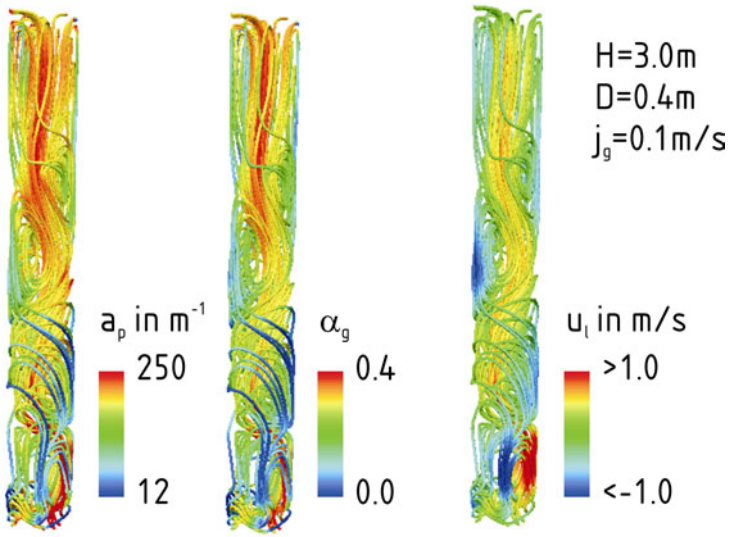

Figure 1: Instantaneous flow field in a bubble column

The flow field is characterized by several large scale vortices in the order of the column diameter. Large values of the interfacial area density are calculated in particular in the core region of the column whereas a low interfacial area is calculated near the walls. The axial liquid velocity reaches from –1.0 to 1.0 m/s. In correspondence with the regions of high gas volume fractions the liquid is transported upwards in the core region and flows downwards near the column walls.

The liquid tracer is injected at the top of the column. In Fig. 2 the time-dependent concentration is shown for two axial positions. In addition the calculated concentrations for several radial positions are also given. Immediately after the injection the tracer is transported downwards in the near wall region. For larger times the tracer is distributed over the whole cross section of the column due to the vortical flow structure. Finally an almost homogeneous distribution of the tracer is reached. The tracer concentration first increases at the upper axial positions 5s after the injection. The tracer concentration reaches a maximum value and then decreases to a constant value. In accordance with its longer distance to the injection point the concentration at the lower position increases later. The concentration increases slowly and reaches the constant value 68 s after the injection. The fluctuations in the concentration increases from the axial position towards the column wall. In particular the fluctuations are damped with increasing time and increasing distance from the injection point.

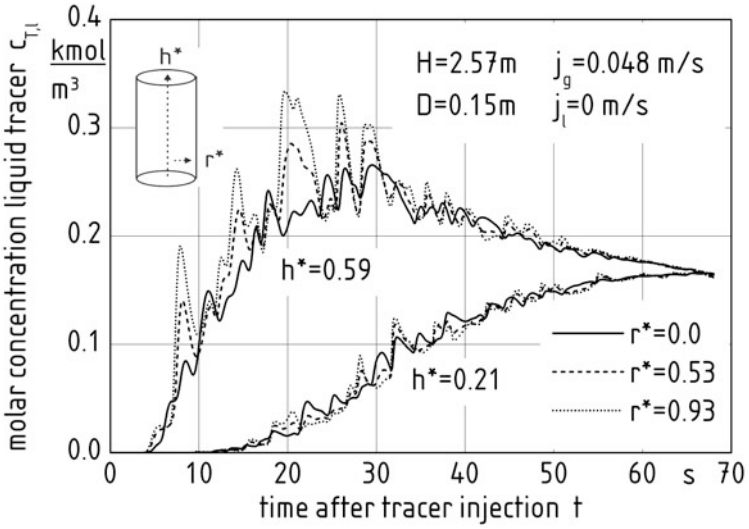

Figure 2: Calculated tracer concentration in the liquid

For comparison with experimental results the axial dispersion model is applied to calculate the axial dispersion coefficients. Therefore the tracer response curves as depicted in Fig. 2 are approximated using eq. (13). The calculated Bodenstein- and Froude-number are shown in Fig. 3. In addition the experimental results of Deckwer [1] are given.

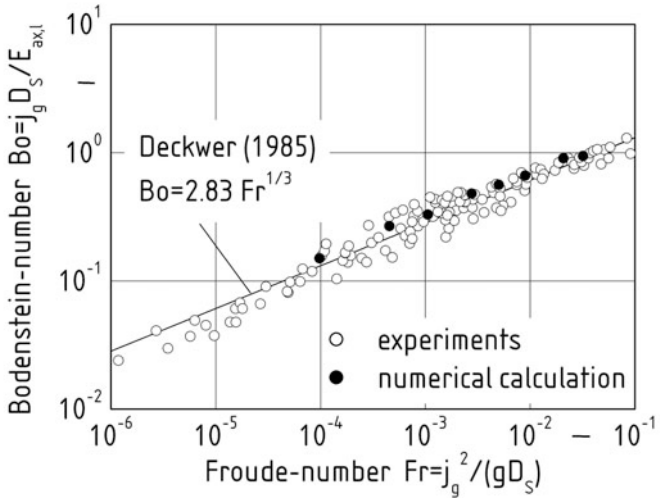

Figure 3: Bodenstein-number vs. Froude-number

With increasing superficial gas velocity the dispersion coefficients increases thus enhanced backmixing in the liquid phase occurs.

The gas tracer is injected continuously into the rising bubbles swarm. The calculations are performed for a cylindrical bubble column in accordance with the experimental investigations of Mangartz and Pilhofer [10]. In Fig. 4 the calculated and experimental dispersion coefficients are shown.

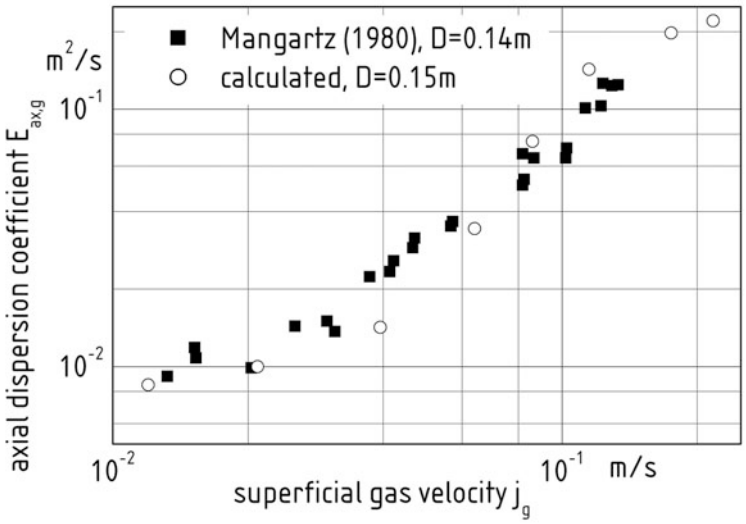

Figure 4: Axial dispersion coefficient for the gas phase

The dispersion coefficients increase with increasing superficial gas velocity. For low superficial gas velocities corresponding to the homogenous flow regime the increase is slighter than in the heterogeneous flow regime. Thus the enhanced formation of vortices and the formation of a bi-modal bubble size distribution significantly influence the mixing properties of the bubble column. The proposed multi-fluid model reasonably predicts the large-scale mixing behavior of bubble columns. Thus the model is extended to include reactive flows.

Therefore the absorption of the gas phase is considered. The calculated flow fields for bubble columns with 2m height and 20cm diameter are shown in Fig. 5 with and without considering mass transfer.

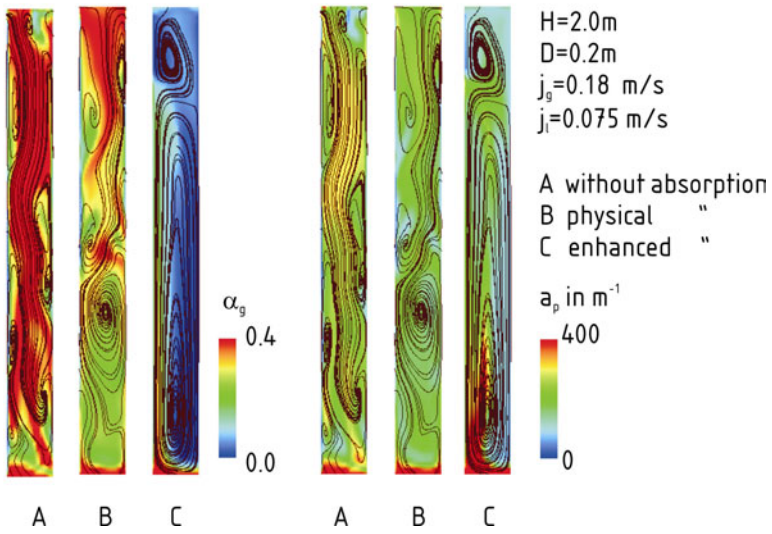

Figure 5: Instantaneous flow fields for several mass transfer rates

The calculations consider two-phase flow without absorption, the physical absorption and the enhanced absorption of the gas phase. The absorption process reduces the volume fraction of gas with increasing column height. The overall gas holdup for the cases A,B and C are 0.318, 0.278 and 0.085. In particular for the case of an enhanced absorption the volume fraction is significantly reduced. The interphase momentum transfer is reduced according to the reduced gas volume fraction. Thus the flow pattern and the specific interfacial area density in the bubble column are changed.

Due to the absorption the bubble diameter decreases. The enhanced absorption significantly changes the bubble diameter as shown in Fig 6.

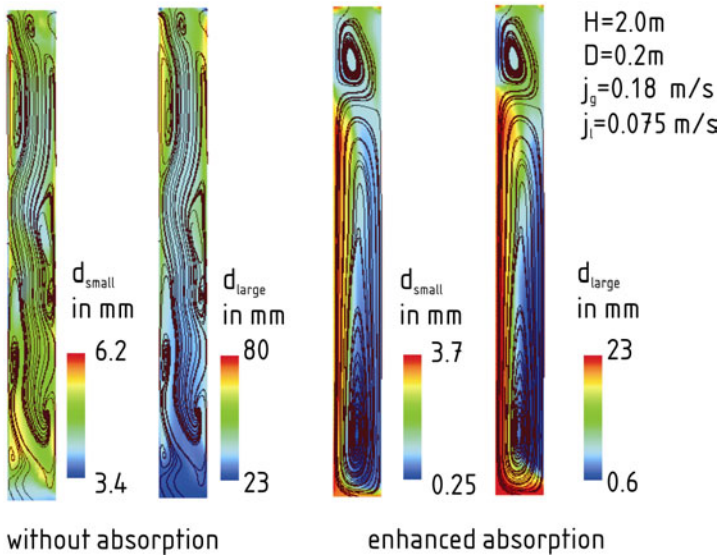

Figure 6: Influence of mass transfer on bubble diameter

The bubble diameter of the large and small bubble fraction are given for the case without mass transfer and for the enhanced absorption. In particular in the downwards flowing part of the circulation loop small bubbles are calculated corresponding with the low gas volume fraction.

Conclusion

A multi-fluid model is applied to calculate three-dimensional, instationary flow fields in bubble columns considering the local bubble size. Therefore the gas phase is decribed by two interpenetrating phases, which represent the small and the large bubble fraction. Considering multiple components in the gas and liquid phase the dispersion of a tracer in both gas and liquid is calculated. As result the time-dependent concentration fields are obtained. For comparison with experimental investigation the axial dispersion coefficients are calculated. The multi-fluid model predicts the axial dispersion coefficients for the gas and liquid phase in good agreement with experimental results. Thus the model is then extended to include mass transfer from the gas to the liquid phase. For large mass transfer rates the reduction of the volume fraction of gas influences the flow pattern significantly.

Acknowledgements

The authors gratefully acknowledge the financial support of the German research Foundation (DFG).
For the calculations the high-performance computer of the North-German High-Performance Computing Combine (HLRN) in Hannover and Berlin is used.

Nomenclature

Latin letters

Symbol	*Units*	*Meaning*
a	m^{-1}	specific area density
c	mol m^{-3}	molar concentration
C_D	-	drag coefficient
d	m	bubble diameter
D	m	column diameter
E	m^2 s-1	dispersion coefficient
Eo	-	Eötvös-number
F	kg m^{-2} s^{-2}	force per unit volume
g	m s^{-2}	gravitational acceleration
H	kg m^{-2} s^{-2}	Henry constant
i,j	-	index
k	m^2 s^{-3}	turbulent kinetic energy
n	-	index
p	kg m^{-2} s^{-2}	pressure
Re	-	Reynolds-number,
Sc	-	Schmidt-number
Sh	-	Sherwood-number
t	s	time
u	m s^{-1}	velocity
x	m	coordinate

Greek letters

Symbol	*Units*	*Meaning*
α	-	volume fraction
β	m s^{-1}	mass transfer coefficient
δ	m	distance
ε	m^2 s^{-3}	turbulent dissipation rate
ζ	-	mass fraction
η	kg m^{-1} s^{-1}	dynamic viscosity
μ	kg $kmol^{-1}$	molar mass
ν	m^2 s^{-1}	kinematic viscosity
π	-	Pi=3.14…
ρ	kg m^{-3}	density
σ	kg s^{-2}	surface tension
ω	s^{-1}	angular frequency

References

[1] W.-D. Deckwer, Bubble column reactors, chap. 6, Verlag Sauerländer, Aarau, 1992

[2] O. Levenspiel, *Chemical Reaction Engineering*, 3rd ed., John Wiley & Sons, New York 1999.

[3] E. Loth, Numerical approaches for motion of dispersed particles, droplets and bubbles, *Prod. Energy Comb. Sci*., vol. 26, pp. 161-223, 2000

[4] J.B. Joshi, V.S. Vitankar, A.A. Kulkarni, M.T. Dhotre, K. Ekambara, Coherent flow structures in bubble column reactors, *Chem. Eng. Sci*., vol. 57, pp. 3157-3183, 2002

[5] R. Clift, J.R. Grace, M.E. Weber, *Bubbles, Drops and Particles*, Academic Press, New York, San Francisco, London 1978.

[6] F. Lehr, M. Millies, D. Mewes, Bubble-size distributions and flow fields in bubble columns, *AIChE J*., vol. 48, pp. 2426-2443, 2002

[7] H. Brauer, Particle/Fluid transport processes, *Prog. Chem. Eng*., vol. 19, pp. 81-11, 1981

[8] M. Lopez de Bertodano, R.T. Lahey, O.C. Jones, Development of a k-ε model for bubbly two-phase flow*, J. Fluids. Eng*., vol. 116, pp. 128-134, 1994

[9] Y. Ohki, H. Inoue, Longitudinal mixing of the liquid phase in bubble columns, Chem. Eng. Sci., vol. 25, pp. 1-16, 1970

[10] K.H. Mangartz, T. Pilhofer, Untersuchungen zur Gasphasendispersion in Blasensäulenreaktoren, *Verfahrenstechnik*, vol. 14, pp. 40-44, 1980